DIMENSIONAL STABILITY OF CURVED PANELS WITH COCURED STIFFENERS AND COBONDED FRAMES[1]

G. E. Mabson, B. W. Flynn , G. D. Swanson
Boeing Commercial Aircraft Group

R. C. Lundquist
Boeing Computer Services

P. L. Rupp
University of Washington

ABSTRACT

Closed form and finite element analyses are presented for axial direction and transverse direction dimensional stability of skin/stringer panels. Several sensitivity studies are presented to illustrate the influence of various design parameters on the dimensional stability of these panels. Panel geometry, material properties (stiffness and coefficient of thermal expansion), restraint conditions and local details, such as resin fillets, all combine to influence dimensional stability, residual and assembly forces.

INTRODUCTION

Composite material structure can show considerable curing-induced dimensional changes. These dimensional changes are primarily the result of coefficient of thermal expansion and stiffness mismatch in the part and/or tool. Resin chemical shrinkage (i.e. resin decrease in volume during cure after it gains some stiffness properties) may also contribute to the problem (Ref. 1). Dimensional changes often cause assembly problems, such as excessive shimming and/or induced residual forces. This paper describes the effort directed toward the prediction of cure-induced dimensional changes associated with composite skin/stringer panels. The intention is to include dimensional change predictions during the design phase of the panel development effort in order to minimize any adverse effects on performance and manufacturing cost.

Material properties of the composite material can vary with temperature and viscoelastic response may also complicate analysis procedures. Flat unstiffened panels fabricated with unsymmetric laminates subjected to temperature changes have been shown to require geometric nonlinear analyses to accurately describe the panel's response (Ref. 2).

---

[1] This work was funded by Contract NAS1-18889, under the direction of J. G. Davis and W. T. Freeman of NASA Langley Research Center

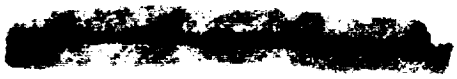

In order to include skin/stringer panel dimensional stability constraints in the optimization program (COSTADE, Ref. 3) being developed in the Boeing ATCAS program, closed form solutions are being developed. The short computational times usually associated with this type of solution should allow the optimizer to operate effectively.

Figure 1 is a photograph of a representative composite skin/stringer panel. The out-of-plane displacements of this panel (Figure 2) show cure induced curvatures along the length of the stiffeners (axial direction) and also transverse to the stiffeners (transverse direction).

The closed form solutions for dimensional stability fall into two categories: axial predictions and transverse predictions.

NOMENCLATURE

a,b,c	constants
A'	classical laminated plate theory A-prime matrix
B'	classical laminated plate theory B-prime matrix
D'	classical laminated plate theory D-prime matrix
E	Young's modulus
F	thermal force resultants, force
g	global
G	thermal moment resultants, shear modulus
i	element number, inner
I	moment of inertia
L	length
M	moment
N	number of elements in cross-section
P	axial load
R	radial direction, radius
s	symmetric
t	total
T	temperature, tangential
u,v	displacements
w	width, displacement
x,y,z	coordinates
$1,2,3$	material principal directions
α	coefficient of thermal expansion
ε	normal strain
γ	shear strain
κ	curvature
ν	Poisson's ratio
θ	angle

Figure 1 Representative Composite Skin/Stringer Panel

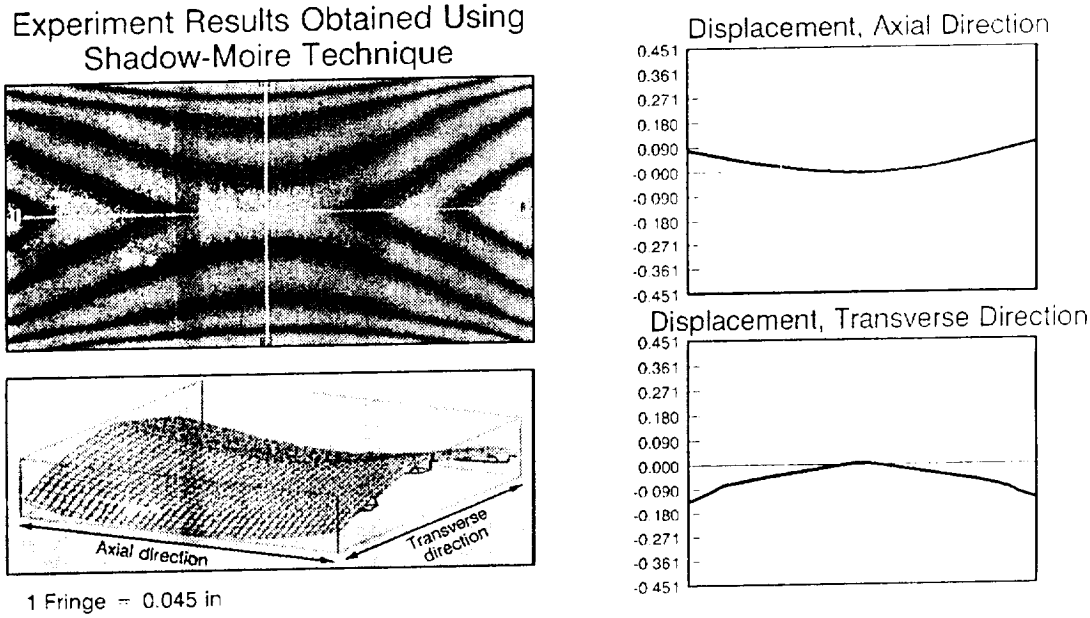

Figure 2 Typical Out-of-Plane Displacements of Representative Skin/Stringer Panels

AXIAL DIRECTION DIMENSIONAL STABILITY

Axial direction dimensional changes can result from stiffener/skin combinations that have axial coefficients of thermal expansion that vary over their cross-section (e.g. different layup in the skin and stiffener). This appears to be the primary cause of axial out-of-plane dimensional changes in skin/stringer panels stiffened in one direction only.

Axial direction dimensional changes can produce waviness in aircraft fuselage structures and therefore can affect aerodynamic properties. Reduced aerodynamic drag may be achieved by designing initial waviness into fuselage panels so that loading during nominal flight conditions counteracts the initial waviness and results in a smooth panel.

Excessive axial dimensional changes may contribute to tool extraction difficulties and the generation of residual forces.

A complex composite beam bending analysis including thermal loading was generated. This analysis was incorporated into a beam bending computer program by adding the coefficient of thermal expansion calculations and thermal loading capabilities. A beam cross-section made from composite material laminates is modelled as an assembly of elements as follows:

1. Each element in the cross-section is straight but may be oriented at an arbitrary angle.
2. Each element in the cross-section obeys classical laminated plate theory. Unbalanced and/or unsymmetric laminates are permissible.
3. Compatibility of axial strain is enforced for all elements in the cross-section. The axial strain is assumed to be bilinear (i.e. $\varepsilon_x = a + b\,y + c\,z$).

This analysis procedure is essentially the same as classical beam theory, modified for composite materials. Appendix A presents the development of this analysis.

Measurements of out-of-plane displacements were performed on sixteen different nominally flat skin/stringer panel configurations at each of three temperatures. These panels incorporated different thicknesses, layups, stringer types, materials and stringer spacings. Closed form and finite element analyses were performed to predict the axial direction results. Figures 3 and 4 present these comparisons for six of the forty-eight different conditions tested.

The finite element analysis used plate elements, small displacements and constant material properties to model the complete panels. Figure 5 presents the skin/stringer panel finite element geometry used. As the closed form solution is based on beam theory, coupling between the transverse and axial directions is not modelled. The finite element plate style model does include this coupling. The closed form and finite element predictions agree to within approximately ten percent.

The test data and predictions compared well for some panel configurations (Figure 3) but not as well for others (Figure 4). Including the effects of variable material properties with temperature, large displacements, chemical shrinkage and "spring in" of curved laminates in the web/skin area may improve the finite element predictions.

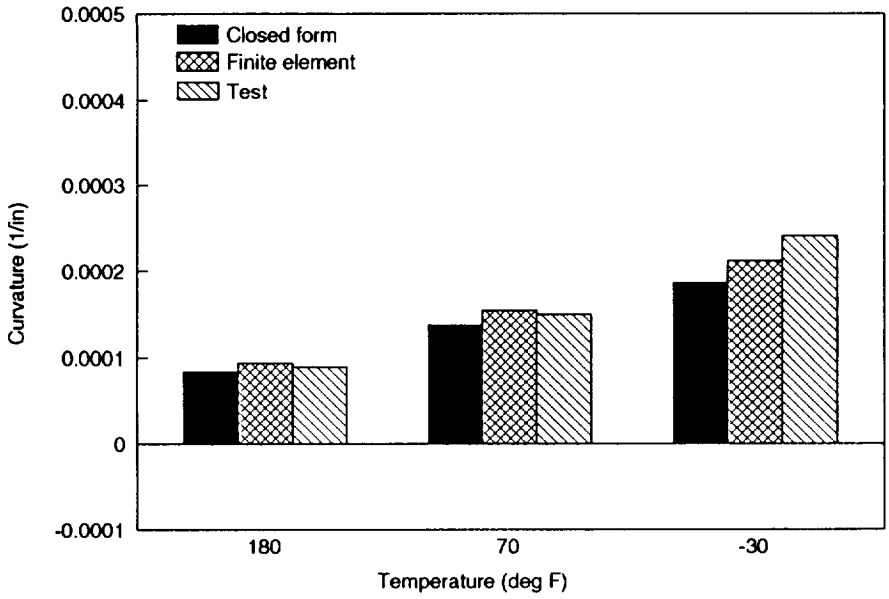

Figure 3 Comparison of Axial Direction Curvature Predictions and Test Data (29-8A)

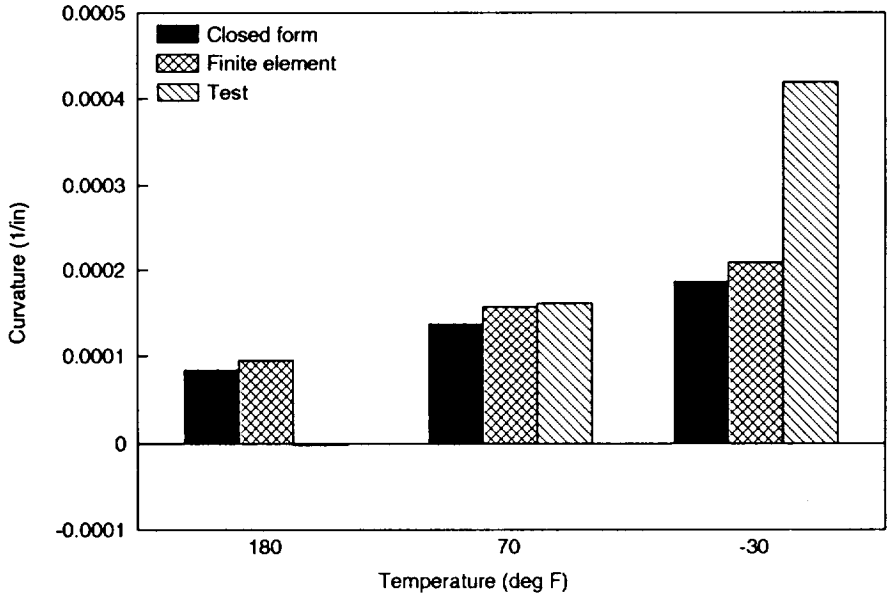

Figure 4 Comparison of Axial Direction Curvature Predictions and Test Data (29-8B)

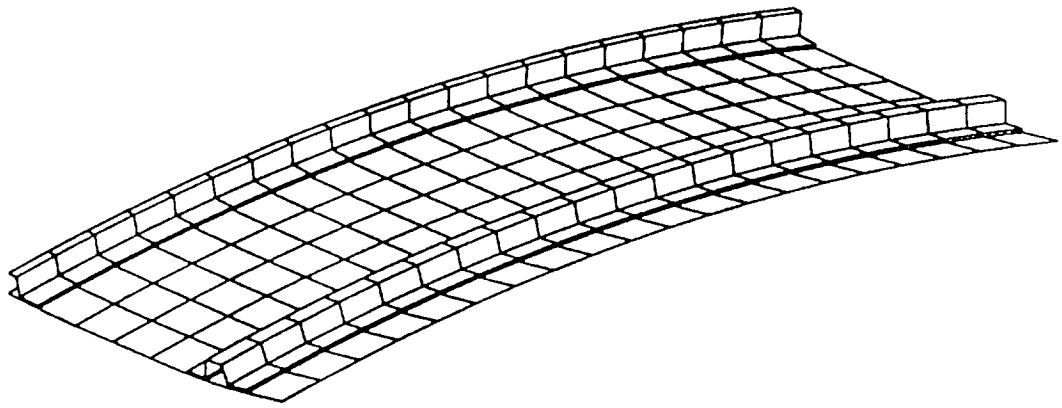

Figure 5 Finite Element Model of Complete Skin/Stringer Panel

Axial Beam Dimensional Stability Sensitivity Studies

Beam Laminate Design Effects

To illustrate the effect of designing beams with elements having different stiffnesses and coefficients of thermal expansion, a sensitivity study on a simple T-section was performed.

The simple T-section, shown in Figure 6, was analyzed for unrestrained thermally induced curvature and for the applied moment required to exactly counteract the curvature (i.e. straightening moment). The laminate in element 2 is held constant as quasi-isotropic $(0/45/-45/90)_s$ AS4[2]/938[3], while the laminate for element 1 is varied. The base laminate for element 1 is also quasi-isotropic; however, the effects of adding additional zero degree plies to its midplane are investigated. Figure 7 presents the unrestrained curvature resulting from a temperature shift. Note that there is an extreme value of curvature when seven additional zero degree plies are added to element 1.

Figure 8 presents the straightening moment for a temperature shift. Note that this straightening moment monotonically increases with additional zero degree plies in element 1. Figures 7 and 8 indicate that element stiffnesses, coefficients of thermal expansion and section geometry all combine to affect thermal curvatures, as well as the straightening moments required to counteract those curvatures.

---

[2] AS4 is a graphite fiber system produced by Hercules, Inc.

[3] 938 is a resin system produced by ICI/Fiberite.

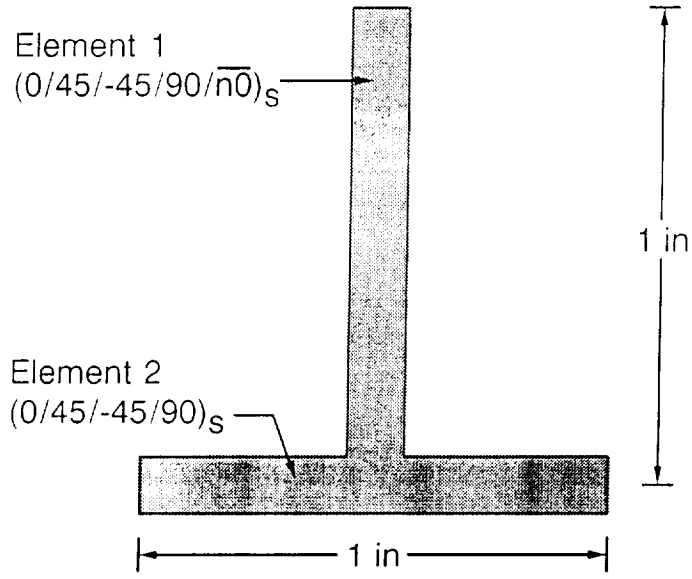

Figure 6 T-Section Beam Geometry

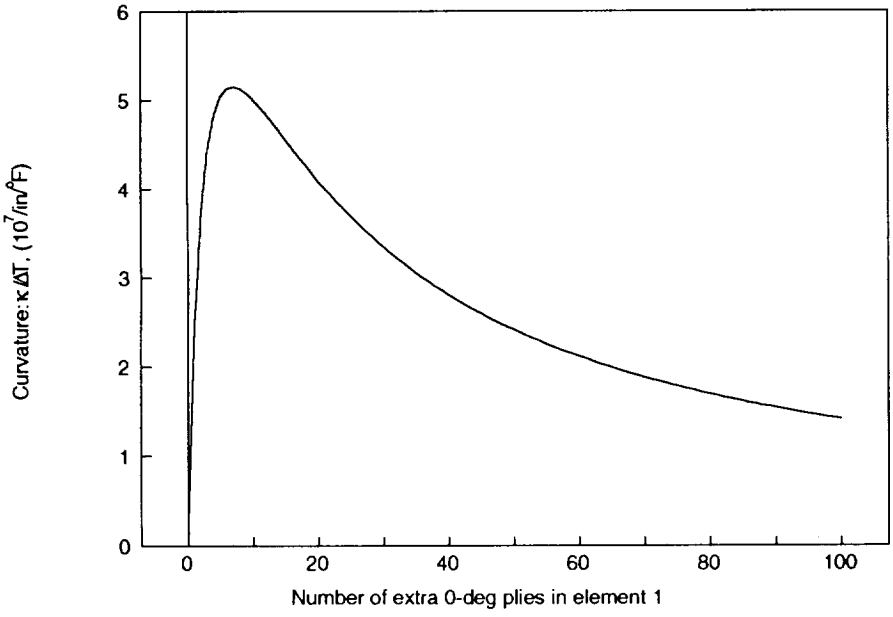

Figure 7 Curvature for T-Section Beam

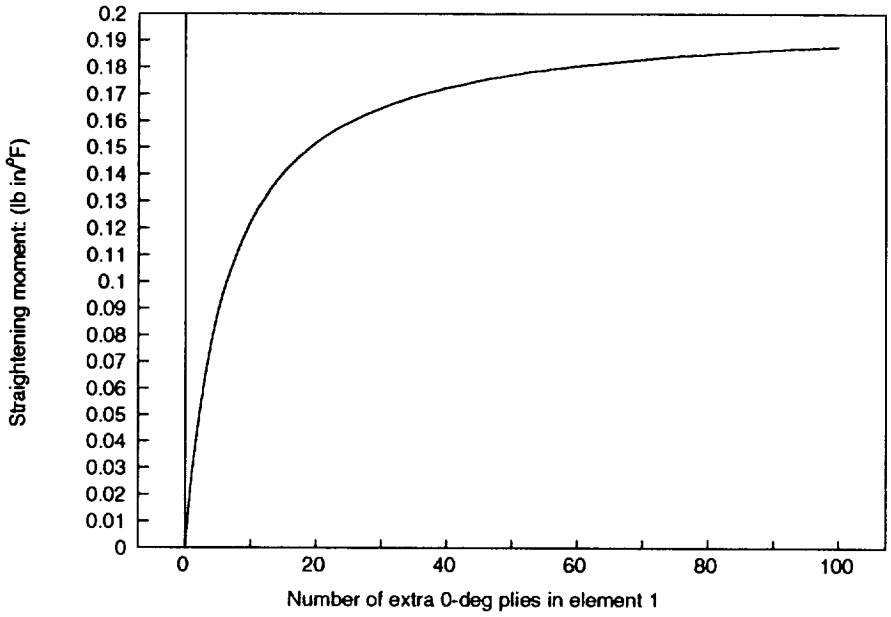

Figure 8 Straightening Moment for T-Section Beam

Beam Support Effects on Dimensional Stability and Assembly Forces

A continuous beam with multiple simple supports was analyzed as a representation of an assembled panel. The supports act as points of attachment as shown in Figure 9. Thermally induced curvature in the beam may result in residual and assembly forces being reacted at the supports. The beam takes the shape shown in Figure 10.

The residual forces are the reaction forces at the supports when the beam is in its final assembled form. If the beam is mechanically fastened to the supports, different support reactions are induced depending upon the order of support attachment. The assembly forces are the reactions induced during assembly. If the beam is attached to all supports simultaneously, in cobonded or cocured structure for example, the support reactions develop as the part cools. In these cases, assembly forces are reduced to be equal to the residual forces.

The maximum magnitude displacements and reaction forces are shown in Figures 11 and 12. Increasing the number of supports decreases the beam displacements at the expense of increasing residual and assembly forces.

Aerodynamic considerations may determine the acceptable out-of-plane displacements of axial panel stiffeners. Beam support strengths may require the residual and assembly forces to be minimized.

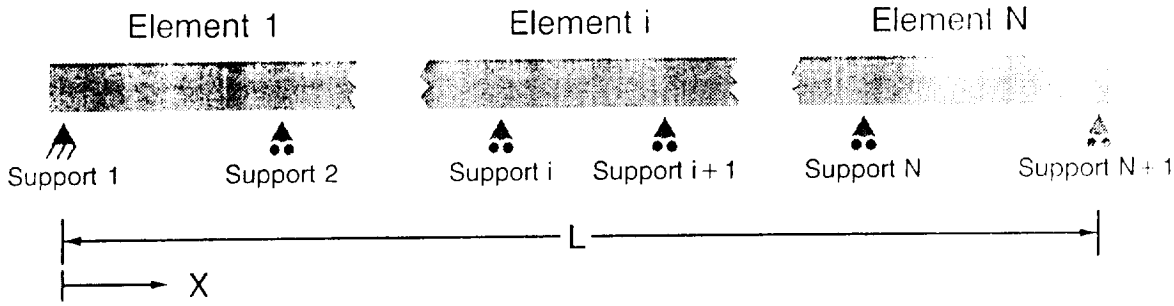

Figure 9 Continuous Beam with Multiple Simple Supports

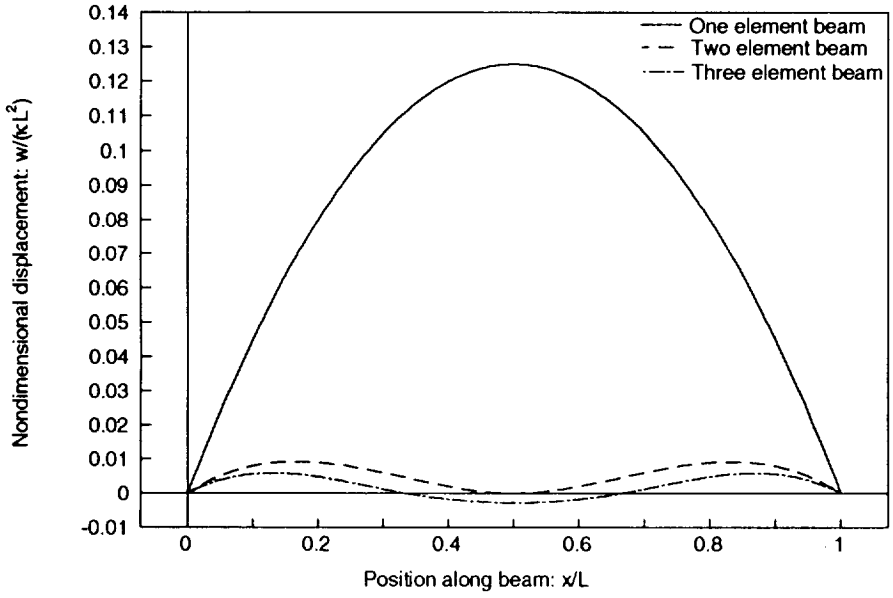

Figure 10 Displacement for Continuous Beams with Multiple Simple Supports

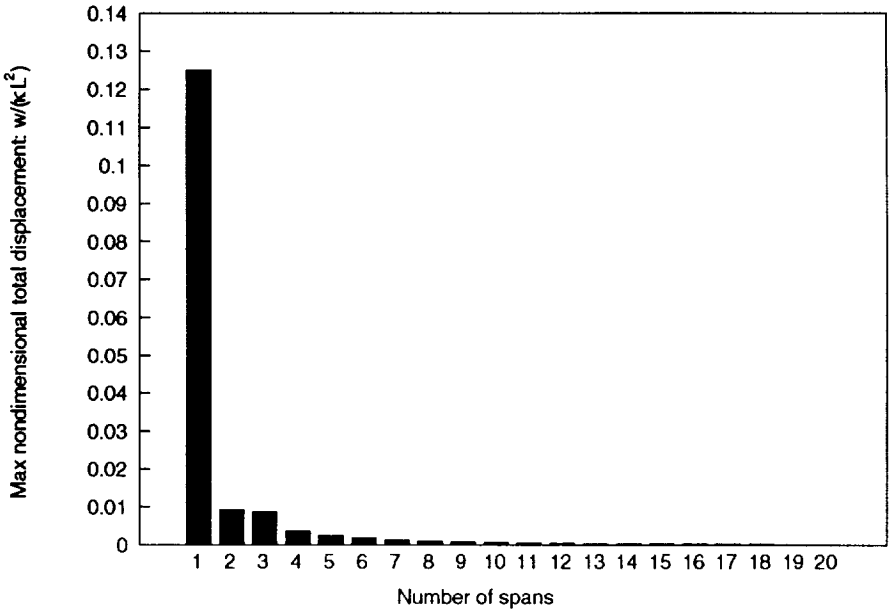

Figure 11 Maximum Out-of-Plane Displacements for Continuous Beams with Multiple Simple Supports

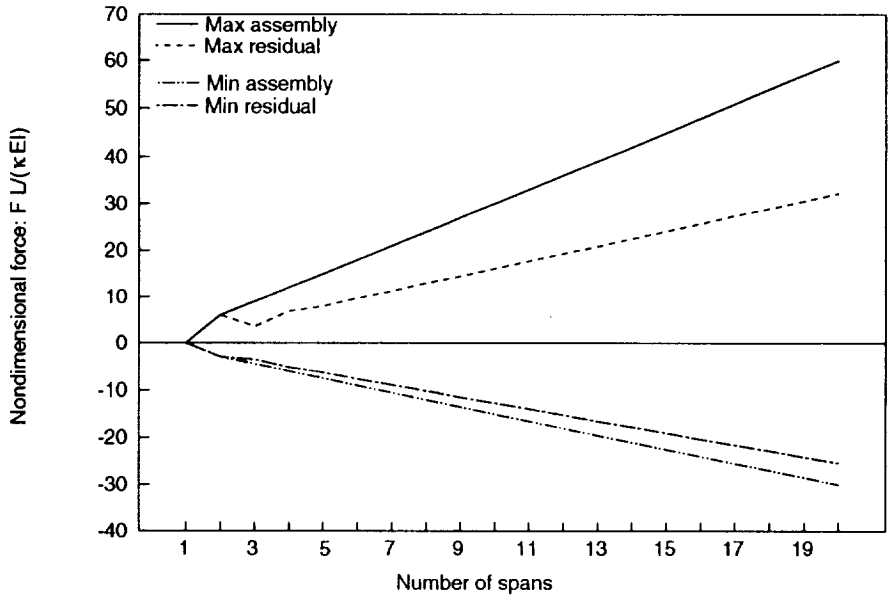

Figure 12 Assembly and Residual Forces for Continuous Beams with Multiple Simple Supports

TRANSVERSE DIRECTION DIMENSIONAL STABILITY

Transverse direction dimensional changes can result from a number of phenomena:

1. Unsymmetrical skins.
2. Unsymmetrical skin/stiffener flange combinations.
3. "Spring in" effect of curved elements at the stiffener/skin interface.
4. Resin pools or fillets.
5. Laminate thickness variations in resin rich or starved areas.

The resin pooling and laminate thickness variations (items 4 and 5 above) can be reduced significantly by modifying the cure tooling. Unsymmetrical skins and skin/stiffener flange combinations may require large displacement theories to accurately describe their response (Ref. 2).

Transverse Direction Dimensional Changes Due to "Spring In"

Symmetric curved composite laminates "spring in" when subjected to a temperature drop (i.e. cure temperature to operating temperature shift). This effect is evident whenever there is a significant difference between the coefficients of thermal expansion in the in-plane and through-the-thickness directions. This phenomenon has caused tool designers to include the effect in the design of tools for fabricating composite parts.

An exact plane strain solution for curved composite laminates subjected to a pure moment or temperature shift is presented in Ref. 4. This analysis solves the equilibrium equations separately in each ply of a laminate, and then assembles the ply solutions together using the appropriate boundary conditions at each ply interface. Stresses, strains and displacements are predicted throughout the laminate. This solution can be used to predict "spring in" angles for arbitrary laminates.

The curved laminate section that joins the stiffener web to the skin/flange combination of a stiffened panel can result in local "spring in" effects. In this situation, the skin and the roving material in the interface will provide some restraint to the curved laminate, as shown in Figure 13. To illustrate this restrained "spring in" phenomenon, an analysis is presented for the 8 ply quasi-isotropic $(0/45/-45/90)_s$ family of laminates for both the skin and curved section. The stacking sequence in both the skin and curved section is varied and "spring in" effects are predicted. Several unsymmetrical laminates were also analyzed for unrestrained "spring in." In this analysis the filler material is ignored. The restraint provided by the skin is assumed to be a pure moment only. The slopes of the skin and curved laminate are forced to be equal where these two laminates join (Figure 13).

The predicted "spring in" angle changes due to a -280°F temperature shift in unrestrained curved laminates are shown in Figure 14. Note that all of the symmetrical laminates are predicted to have virtually the same "spring in." The simple equation (see Equation *1* below) for the homogeneous single ply case compares quite well with the exact plane strain solution for symmetrical laminates. Note that the laminate value of α_R, rather than the lamina value α_3, is used.

$$\textit{"Spring in" angle} = \theta\, \Delta T\, (\, \alpha_T - \alpha_R\,) \qquad (1)$$

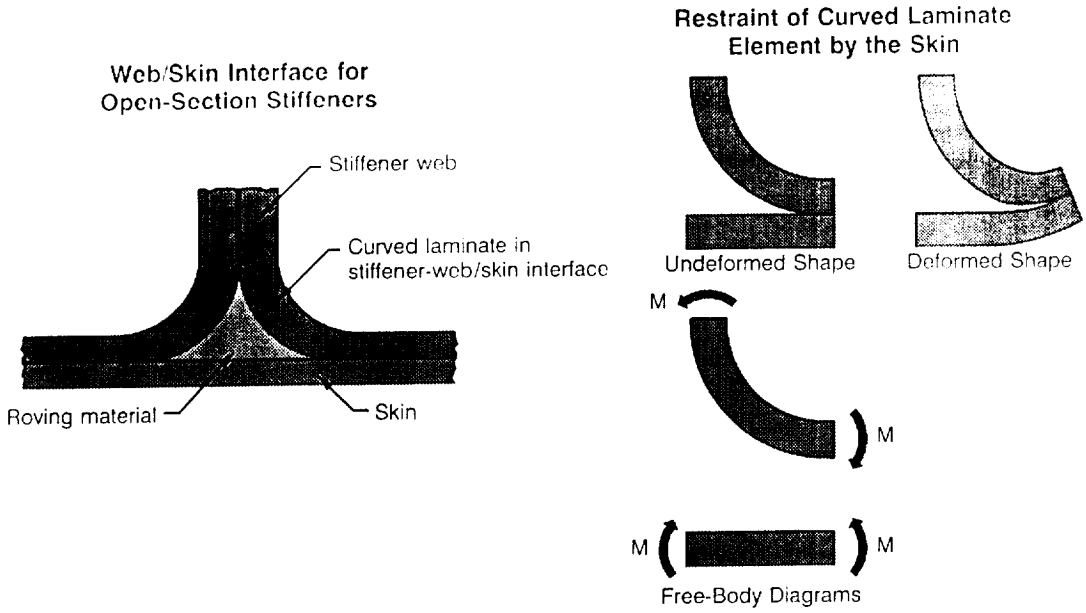

Figure 13 Stiffener Web/Skin Interface

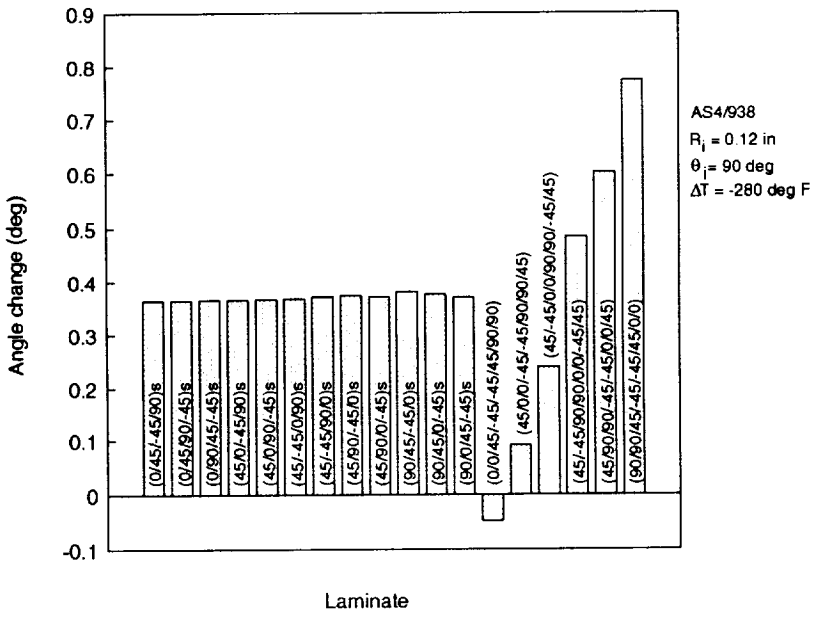

Figure 14 Stacking Sequence Effect on "Spring In" Angle Change for Unrestrained Curved Laminate

Note that unsymmetrical laminates can cause drastic changes in "spring in" response. "Spring out" can be induced in this manner. Ref. 5 presents a design of an aircraft leading edge using unsymmetrical laminates to control "spring in" effects.

The "spring in" angle change due to a -280°F temperature shift when a $(0/45/-45/90)_s$ and a $(90/45/-45/0)_s$ skin laminate provide restraint is shown in Figures 15 and 16, respectively. The ply stacking sequences of these quasi-isotropic skin laminates significantly affects the predicted "spring in" associated with the stiffener web/skin interface.

The angle change predictions presented are based on constant material properties and small displacements. Chemical shrinkage has not been included here. The effective stress-free temperature used in the analysis was the cure temperature. Additional material property evaluations and improved boundary conditions are necessary to refine this analysis.

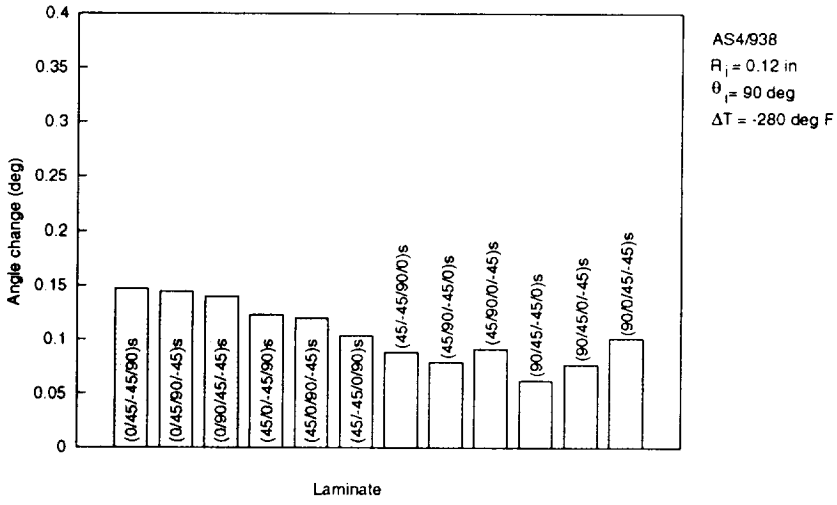

Figure 15 Stacking Sequence Effect on Angle Change for $(0/45/-45/90)_s$ Skin Restraint

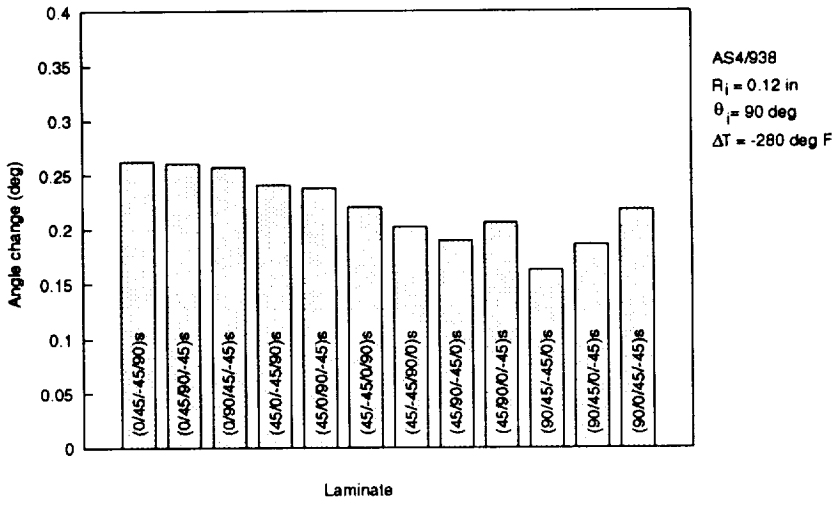

Figure 16 Stacking Sequence Effect on Angle Change for $(90/45/-45/0)_S$ Skin Restraint

Closed Section Stiffener Transverse Direction Dimensional Changes

A closed form solution was developed to model the transverse direction dimensional changes of hat section stiffeners. The hat section is modelled as an assembly of straight and curved elements as shown in Figure 17. Plane strain conditions are imposed in the *x-y* plane (i.e., $\varepsilon_z = \gamma_{xz} = \gamma_{yz} = 0$). The straight elements are assumed to obey classical laminated plate theory. For the curved elements, the plane strain solution (Ref. 4) is used for the pure moment and temperature shift, whereas classical laminated plate theory is used for the axial loading and varying moment. Slope and displacement compatibility is enforced at element interfaces. External temperature shifts provide the loading. Appropriate boundary conditions are applied to the left ends of elements 1 and 2 to enforce symmetric response of the overall cross-section.

This closed form solution was validated by comparing its predictions with a finite element analysis. In the finite element analysis, each ply was modelled with a separate solid element using ABAQUS (Ref. 6). Plane strain conditions were imposed by applying the appropriate boundary conditions. The closed form and finite element predictions compare favorably as shown in Figure 18.

Measurements were obtained on the skin of a section of a hat stiffener. Figure 19 presents the closed form predictions and test data. Both thermal and chemical shrinkage effects are included in the predictions. The temperature shift used was simply the difference between the cure temperature and the test temperature. The chemical shrinkage value used ($\varepsilon_1 = 0, \varepsilon_2 = \varepsilon_3 = -0.0015$) was taken from Reference 1. Reasonable agreement of the analysis and test data is indicated.

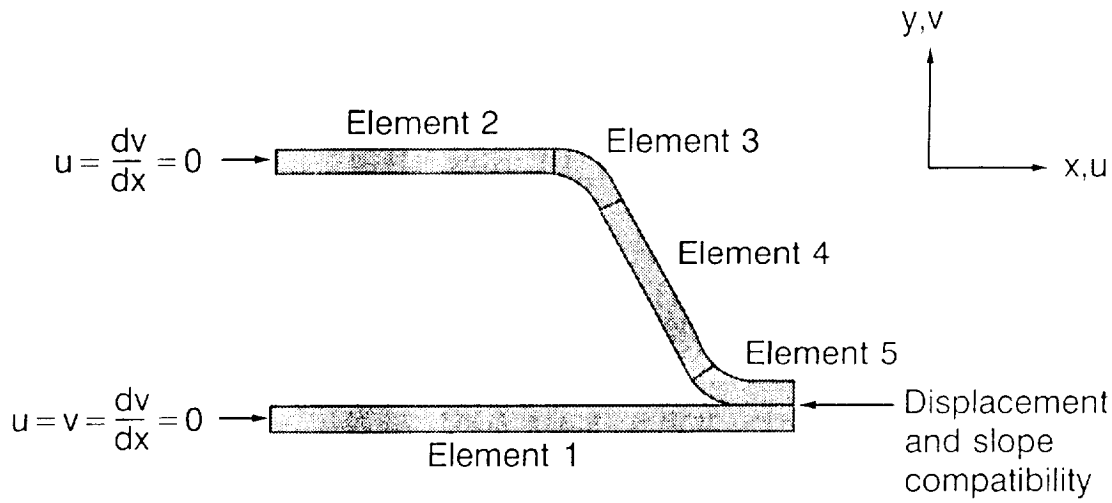

Figure 17 Hat Section Closed Form Solution Model

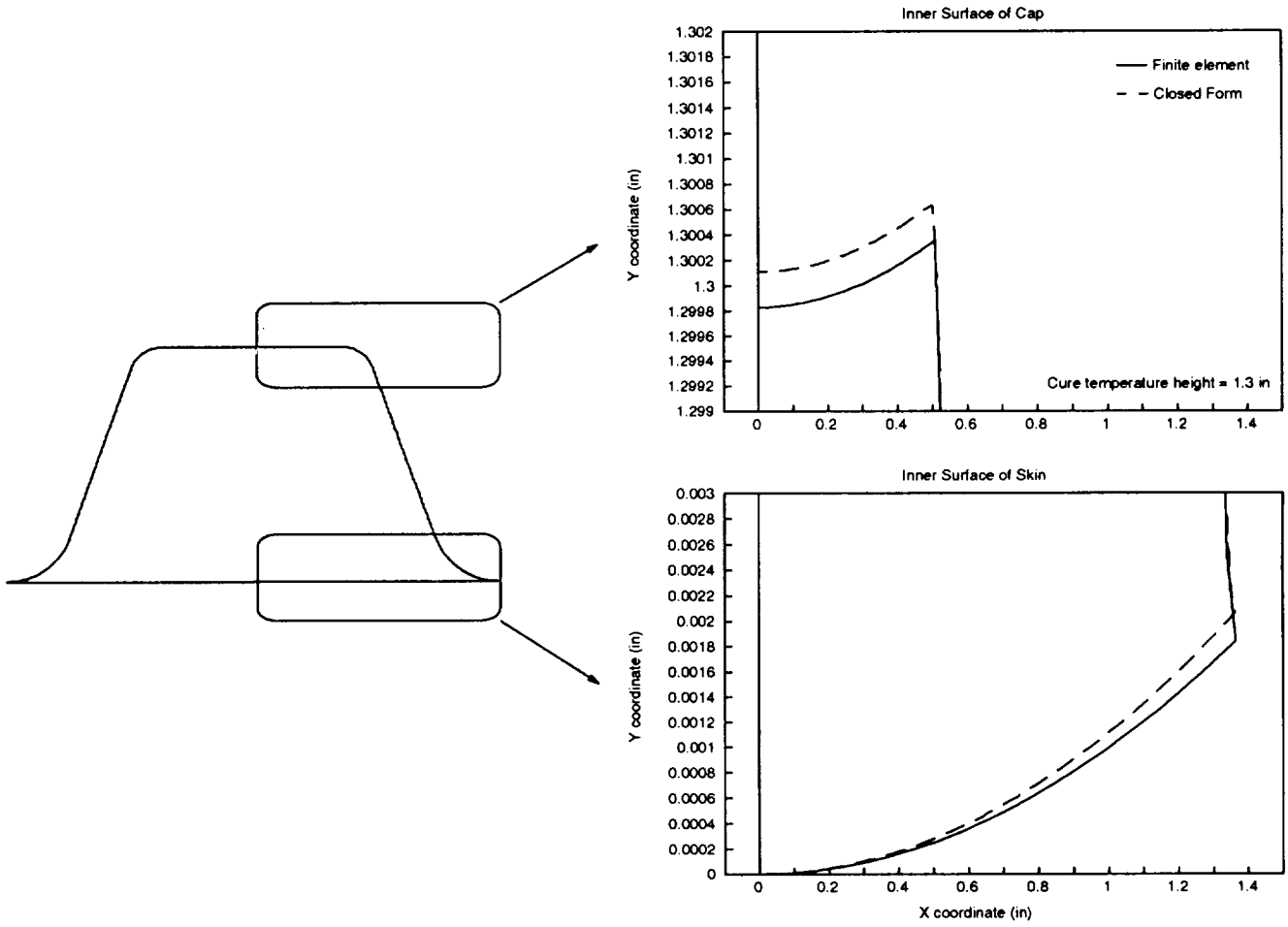

Figure 18 Comparison of Closed Form and Finite Element Analyses for Transverse Direction Dimensional Stability of Hat Sections (Ambient Conditions)

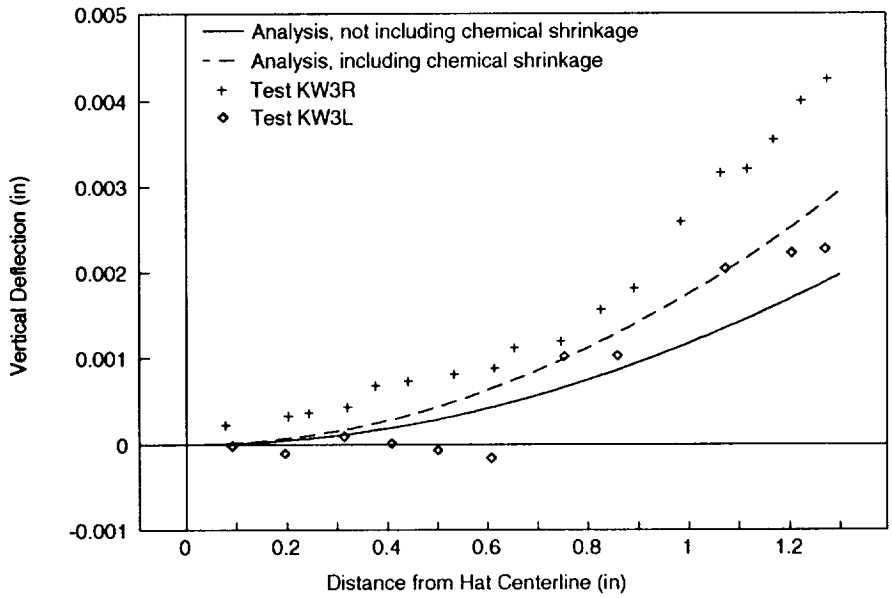

Figure 19 Hat Section Skin Deformation Analysis and Test Comparison (Ambient Conditions)

Mandrel Extraction Analysis

In an effort to understand the difficulties encountered in removing layered aluminum mandrels from certain Boeing ATCAS hat stiffeners, finite element models of the hat section, with and without the resin fillet shown in Figure 20, were performed.

Predictions of the aluminum mandrel position were also made. Results of these analyses are presented in Figures 21 and 22. Note the dramatic influence of the fillet on the deformation of the cross-section. The "no resin fillet" model predicts no interference between the mandrel and hat. The model that includes the resin fillet predicts interference on elements 2 through 4. This appears to be a major contributor to the mandrel extraction problems encountered. Dimensional changes in the axial direction may also have aggravated the mandrel extraction problems.

CONCLUSIONS

Closed form and finite element analyses have been presented for axial direction and transverse direction dimensional stability of skin/stringer panels.

Section geometry, material properties (stiffness and coefficient of expansion) and restraint conditions all combine to influence axial direction dimensional stability and residual and assembly forces. Mechanically attached stiffeners induce larger assembly forces than similar cocured or cobonded ones.

Unsymmetrical laminates may be used to control "spring in" in unrestrained curved laminates. The ply stacking sequences of laminates significantly affect the "spring in" response for restrained curved laminates.

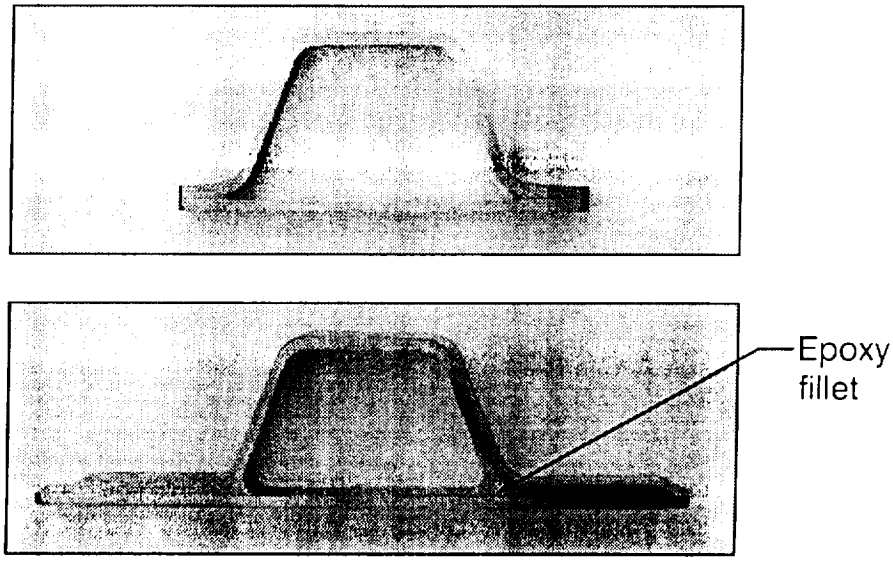

Figure 20 Photograph of Hat Section Stiffener Without and With Fillet

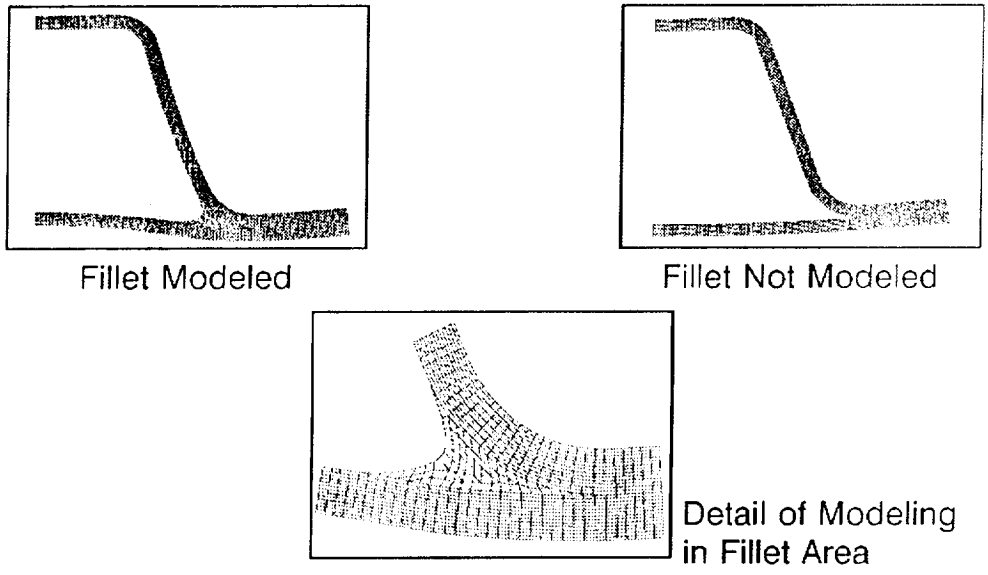

Figure 21 Plane Strain Finite Element Model Results for Hat Section Stiffener Cross-Sections (Amplified Displacements for Ambient Conditions)

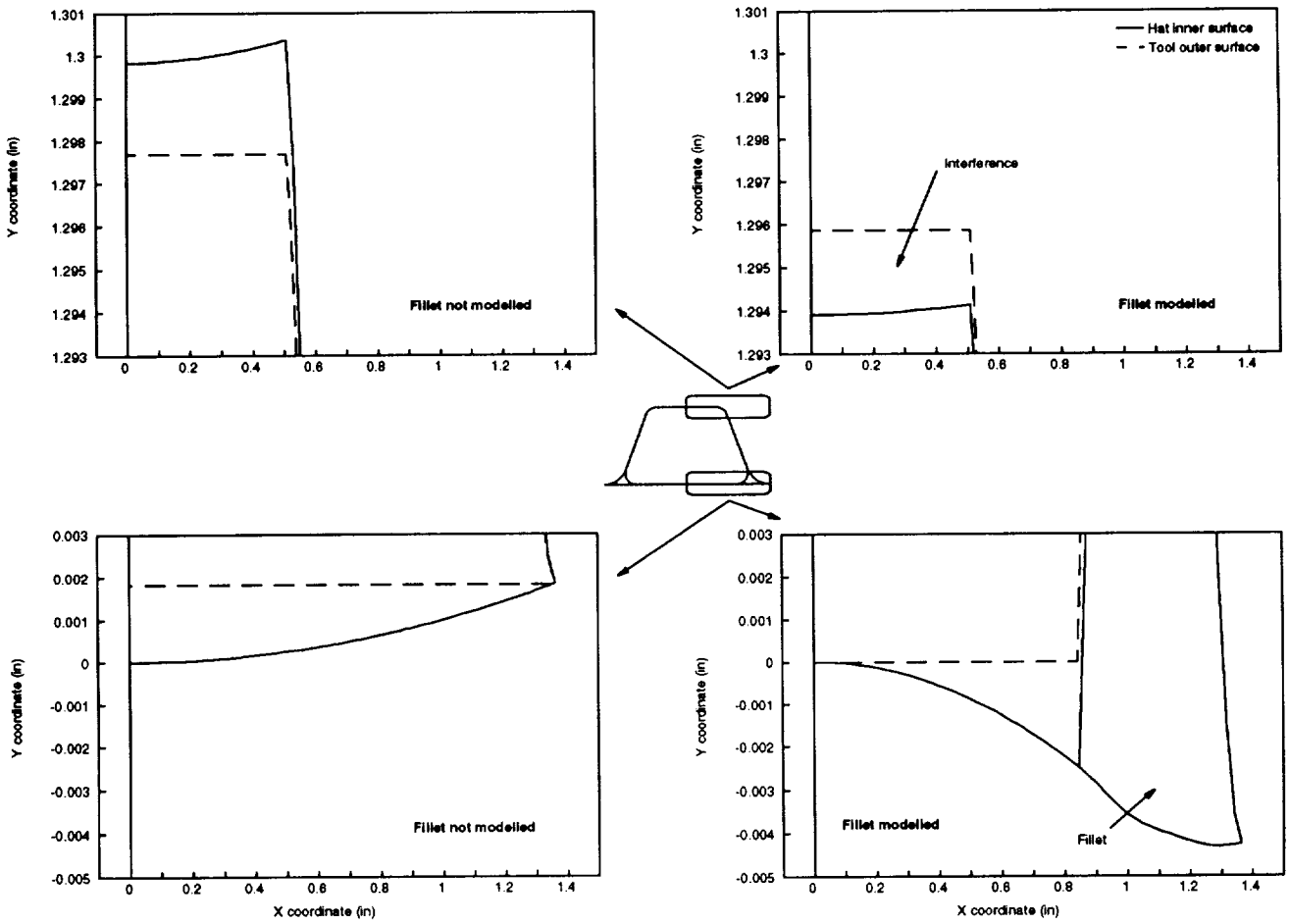

Figure 22 Effect of Fillet on Transverse Direction Dimensional Stability and Tool Extraction for Hat Section Stiffeners (Ambient Conditions)

Resin fillets have a drastic influence on transverse direction dimensional stability.

Closed form analyses compare well with small displacement, constant material property finite element analyses for both axial and transverse direction dimensional stability predictions.

Further work is required in the following areas:

1. Large displacement finite element modelling of skin/stringer panels.
2. Nonconstant material property finite element modelling.
3. Include transverse direction "spring in" in finite element complete panel models.
4. Generate chemical shrinkage, effective stress-free temperature material properties.
5. Include dimensional stability analyses into COSTADE.
6. Further investigation of dimensional stability issues caused by tool/part coefficient of thermal expansion mismatch.

REFERENCES

1. Nelson, R. H. and Cairns, D. S.: *Prediction of Dimensional Changes in Composite Laminates During Cure*, 34th International SAMPE Symposium, May 8-11, 1989, pp. 2397-2410.

2. Hyer, M. W.: *Some Observations on the Cured Shape of Thin Unsymmetric Laminates*, Journal of Composite Materials, Vol. 15, 1981, pp 175.

3. Freeman, W. T., Ilcewicz, L. B., Swanson, G. D. and Gutowski, T.: *Designer's Unified Cost Model*, Proceedings of the Ninth DoD/NASA/FAA Conference on Fibrous Composites in Structural Design, FAA Publication, 1991.

4. Mabson, G. E. and Neall, E. P.: *Analysis and Testing of Composite Aircraft Frames for Interlaminar Tension Failure*, Presented at the National Specialist's Meeting on Rotary Wing Test Technology of the American Helicopter Society, Bridgeport, Connecticut, Mar. 15-16, 1988.

5. Nolet, S. C. and Sandusky, P. M.: *Impact Resistant Hybrid Composite For Aircraft Leading Edges*, SAMPE Quarterly, Vol. 17, No. 4, July 1986, pp. 46-53.

6. *ABAQUS User's Manual Version 4.8.* Copyright 1989 by Hibbitt, Karlsson & Sorensen Inc.

APPENDIX A

COMPOSITE BEAM SECTION ANALYSIS INCLUDING THERMAL LOADING

The response of a single element is modelled as shown in Figure A1. Note that the element coordinate system origin ($y = 0, z = 0$) chosen is the location where no x-direction curvature results due to axial loads on the element (i.e. $B_{11}' = 0$). This location is the element midplane for symmetric laminates.

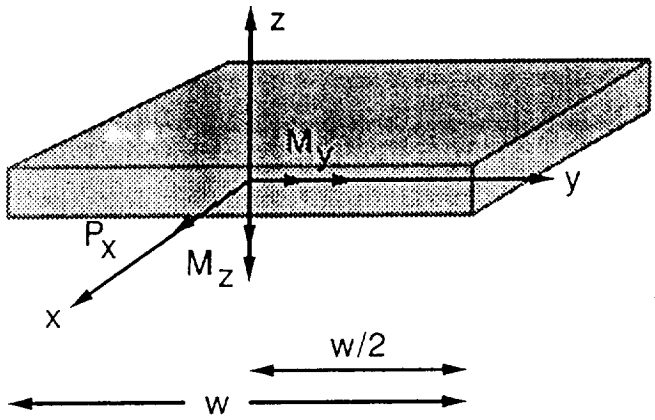

Figure A1 Element Coordinate System and Loading

The axial strain for an element due to the load and moments (P_x, M_y, M_z) and thermal loading in the element coordinate system is

$$\begin{aligned}\varepsilon_x = \; & A_{11}' P_x / w + A_{11}' F_1 + A_{12}' F_2 + A_{16}' F_3 + B_{12}' G_2 + B_{16}' G_3 \\ & + y\, 12\, A_{11}' M_z / w^3 \\ & + z\,(D_{11}' M_y / w + B_{21}' F_2 + B_{61}' F_3 + D_{11}' G_1 + D_{12}' G_2 + D_{16}' G_3) \end{aligned} \qquad (A1)$$

For a multi-element cross-section, Figure A2 illustrates the global coordinate system used. The total load and moments about the global coordinate system origin ($y_g = 0$, $z_g = 0$) are

$$P_{xt} = \sum_{i=1}^{N} P_{xi} \qquad (A2)$$

$$M_{yt} = \sum_{i=1}^{N} (M_{yi} \cos \theta_i + M_{zi} \sin \theta_i + P_{xi} z_i) \qquad (A3)$$

$$M_{zt} = \sum_{i=1}^{N} (M_{zi} \cos \theta_i - M_{yi} \sin \theta_i + P_{xi} y_i) \qquad (A4)$$

For arbitrary loads (P_{xt}, M_{yt}, M_{zt} and thermal) applied to the cross-section at the global origin, the unknowns are the element loads P_{xi}, M_{yi}, M_{zi} (in each element coordinate system) and the axial strain constants a, b and c where

$$\varepsilon_x = a + b\, y_g + c\, z_g \qquad (A5)$$

The above equation is written with respect to the global coordinate system.

This results in $3N+3$ unknowns.

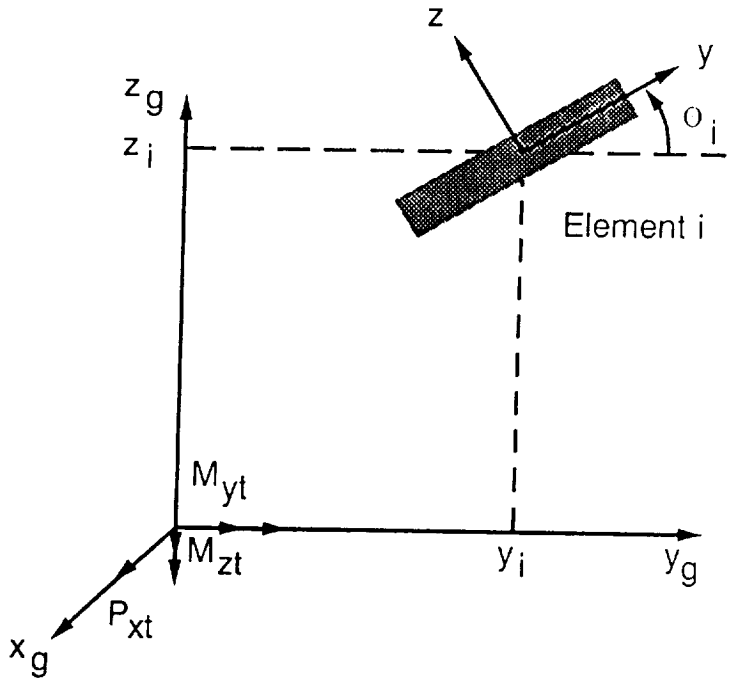

Figure A2 Global Coordinate System and Loading

The equations to be solved are equations *A2*, *A3* and *A4* and for each element:

$$
\begin{aligned}
a = \; & A_{11}' P_{xi} / w_i + A_{11}' F_1 + A_{12}' F_2 + A_{16}' F_3 + B_{12}' G_2 + B_{16}' G_3 \\
& + y_i (-12 A_{11}' M_{zi} \cos \theta_i / w_i^3 \\
& + (B_{21}' F_2 + B_{61}' F_3 + D_{11}' M_{yi} / w_i + D_{11}' G_1 + D_{12}' G_2 + D_{16}' G_3) \sin \theta_i) \\
& + z_i (-12 A_{11}' M_{zi} \sin \theta_i / w_i^3 \\
& - (B_{21}' F_2 + B_{61}' F_3 + D_{11}' M_{yi} / w_i + D_{11}' G_1 + D_{12}' G_2 + D_{16}' G_3) \cos \theta_i) \qquad (A6)
\end{aligned}
$$

$$
\begin{aligned}
b = \; & 12 A_{11}' M_{zi} \cos \theta_i / w_i^3 \\
& - (B_{21}' F_2 + B_{61}' F_3 + D_{11}' M_{yi} / w_i + D_{11}' G_1 + D_{12}' G_2 + D_{16}' G_3) \sin \theta_i \qquad (A7)
\end{aligned}
$$

$$
\begin{aligned}
c = \; & 12 A_{11}' M_{zi} \sin \theta_i / w_i^3 \\
& + (B_{21}' F_2 + B_{61}' F_3 + D_{11}' M_{yi} / w_i + D_{11}' G_1 + D_{12}' G_2 + D_{16}' G_3) \cos \theta_i \qquad (A8)
\end{aligned}
$$

This results in *3N+3* equations.